

UC San Diego

UC San Diego Previously Published Works

Title

Aqueous Angiography in Living Nonhuman Primates Shows Segmental, Pulsatile, and Dynamic Angiographic Aqueous Humor Outflow.

Permalink

<https://escholarship.org/uc/item/8hq1769r>

Journal

Ophthalmology, 124(6)

Authors

Huang, Alex
Li, Meng
Yang, Diya
et al.

Publication Date

2017-06-01

DOI

10.1016/j.optha.2017.01.030

Peer reviewed



HHS Public Access

Author manuscript

Ophthalmology. Author manuscript; available in PMC 2018 June 01.

Published in final edited form as:

Ophthalmology. 2017 June ; 124(6): 793–803. doi:10.1016/j.ophtha.2017.01.030.

Aqueous Angiography in Living Non-Human Primates Show Segmental, Pulsatile, and Dynamic Angiographic Aqueous Humor Outflow

Alex S. Huang^{1,*}, Meng Li², Diya Yang², Huaizhou Wang², Ningli Wang^{2,*}, and Robert N. Weinreb³

¹Doheny Eye Institute, Los Angeles, CA; Department of Ophthalmology, David Geffen School of Medicine at UCLA, Los Angeles, CA

²Beijing Institute of Ophthalmology, Beijing Tongren Eye Center, Beijing Tongren Hospital, Capital Medical University, Beijing, China

³Hamilton Glaucoma Center and Shiley Eye Institute, University of California, San Diego, CA

Abstract

Purpose—To evaluate the feasibility of safely performing aqueous angiography in intact eyes of living non-human primates (NHPs) for evaluating aqueous humor outflow and segmental patterns.

Methods—Aqueous angiography was performed in 6 non-human primates. After anesthesia, an anterior chamber (AC) maintainer was placed through a temporal 1 mm side-port wound. Indocyanine green (ICG; 0.4%) or 2.5% fluorescein was introduced (individually or in sequence) into the eye with a gravity-driven constant-pressure system. Aqueous angiography images were obtained with a Spectralis HRA+OCT (Heidelberg Engineering) suspended over the NHP eye using a custom designed surgical boom arm. Concurrent anterior segment optical coherence tomography (OCT) was performed on distally angiographically positive and negative regions.

Results—Aqueous angiography in the living NHP eye demonstrated mostly stable angiographic patterns. With multi-modal imaging, angiographically positive signal co-localized with episcleral veins as identified by infrared imaging and intrascleral lumens as demonstrated by anterior segment OCT. Sequential aqueous angiography in individual eyes with ICG followed by fluorescein showed similar angiographic patterns. A pulsatile nature of aqueous angiographic outflow was sometimes observed. Aqueous angiographic patterns could also dynamically change. In some instances, positive angiographic flow suddenly arose in regions previously without angiographic signal. Alternatively, angiographic signal could suddenly disappear from regions in which angiographic signal was initially documented.

*Co-Corresponding Authors: Alex Huang, MD/PhD, Doheny Eye Institute, Department of Ophthalmology, David Geffen School of Medicine, University of California, Los Angeles, 1355 San Pablo Street, Los Angeles, CA 90033, Ahuang@Doheny.org, Phone: 323-442-6436; Fax: 323-442-6688. Ningli Wang MD/PhD, Beijing Tongren Eye Center, Beijing Tongren Hospital, Capital Medical University, Beijing, Beijing, China, wningli@vip.163.com, Phone +86 131 2146 3355; Fax: +86 10 5826 9930.

Publisher's Disclaimer: This is a PDF file of an unedited manuscript that has been accepted for publication. As a service to our customers we are providing this early version of the manuscript. The manuscript will undergo copyediting, typesetting, and review of the resulting proof before it is published in its final citable form. Please note that during the production process errors may be discovered which could affect the content, and all legal disclaimers that apply to the journal pertain.

Discussion—Aqueous angiography in living NHPs demonstrated segmental and pulsatile patterns with a newly described ability to dynamically shift. These characteristics further the understanding of live aqueous humor outflow biology and maybe useful in improving glaucoma surgeries aimed at trabecular meshwork bypass.

Introduction

A better understanding of the complete conventional aqueous humor outflow (AHO) pathway is necessary. For good reason, traditional AHO investigations have focused on the trabecular meshwork (TM) because it was identified as the primary resistor to AHO in the eye^{1, 2}. Moreover, glaucomatous eyes showed increased resistance at the level of the TM^{1, 2}. However, it was apparent that there was also post-TM³ outflow resistance which was further increased in glaucoma compared to normal eyes^{1, 4}. These basic observations coupled with the clinical results of variable success in IOP lowering with surgical trabecular bypass in human glaucoma patients have suggested that the full nature of AHO is more complex and warrants further study⁵⁻⁸.

Structural evaluation of AHO pathways has improved with the advent of optical coherence tomography (OCT)⁹⁻¹¹. The TM has been hypothesized to be represented by an interphase shadow⁹, and Schlemm's Canal (SC) and distal outflow lumens show low reflectivity on anterior segment OCT. Three-dimensional reconstructions of distal outflow pathways have been created in-whole in post-mortem model enucleated eyes¹² or in-part in live normal human subjects¹⁰. Automated segmentation algorithms are under development (Dastiridou, A et al. IOVS 2016; ARVO Abstract 5119-C0134). In particular, phase-based OCT has shown dynamic motion in TM and post-TM outflow pathways with demonstration of a pulsatile tempo likely related to the cardiac cycle¹³⁻¹⁷.

Aqueous angiography is a recently developed method to visualize functional AHO as real-time imaging of tracer movement¹⁸⁻²¹. In post-mortem pig, cow, and human eyes, similar patterns can be visualized using multiple tracers such as fluorescein or indocyanine green (ICG)¹⁸⁻²¹. Segmental patterns have been observed that may be relevant to trabecular bypass surgeries and their success via concepts of guiding surgical placement toward areas of greater or lesser flow in the eye. Comparisons between ICG and fluorescein aqueous angiography have shown sufficient similarity to conduct interventional studies where ICG is first used to determine a pattern followed by fluorescein after an intervention to query the effect^{19, 20}. With this method, regions of initially poor angiographic flow have been shown to be capable of angiographic recruitment for enhanced flow using aqueous angiography-guided trabecular bypass in enucleated human eyes²⁰. Limitations translating aqueous angiographic investigations of enucleated eyes to *in vivo* ones include post-mortem cellular necrosis, potential presence of episcleral venous blood clots, and the discontinuation of the episcleral vein from the systemic venous circulation leading to tracer accumulation on the ocular surface.

Therefore, we conducted real-time aqueous angiography for the first time in intact eyes using living non-human primates (NHP A-F). Qualitative observations confirmed a

segmental and pulsatile nature of AHO. The observation that AHO patterns could dynamically change in a living eye was a novel discovery.

Methods

Test Subjects

This study was carried out in accord with the Declaration of Helsinki, the ARVO Statement for the Use of Animals in Ophthalmic and Vision Research, and in approval by the Institutional Animal Care and Use committee (IACUC) of Beijing Institute of Xieerxin Biology Resource. Rhesus macaque monkeys (NHP; *Macaca mulatta*) involved in this study were all purchased from Beijing Institute of Xieerxin Biology Resource, which is one of the largest NHP centers in the northern part of China. They specialize in breeding laboratory NHPs for studies routinely done through Beijing Tongren Hospital and Capital Medical University. Six adult (5 males and 1 female) NHPs were used (Table 1). They had a mean weight of 9.65 kg (range 7.5–12.3 kg) and mean age of 15.5 years (range 10–25 years). Each NHP was chosen by pre-examination of the eyes at cage-side to identify animals with minimal conjunctival pigmentation. Imaging of the animals was done at the Beijing Institute of Xieerxin Biology Resource in a dedicated procedure room. The NHPs were individually housed at a temperature of 16–28°C. Feeding regimens were standard animal feeds involving various kinds of vegetables and fruits. No NHP that participated in this study was sacrificed.

The animals were anesthetized with Zoletil 50 (Tiletamine/Zolazepam; Laboratorios Virbac, Bogota, Colombia, S.A.). The initial dose was 5 mg/kg intramuscular for each NHP²². Inhalational general anesthesia was not used as the mask size precluded the imaging device from coming close enough to obtain images. The NHPs were then secured to the procedure table with soft restraints similar to those used in human surgeries. Topical 0.5% proparacaine hydrochloride (Alcaine; Alcon Laboratories, Forth Worth, TX) was applied, and the eye was sterile prepped with entoiodine swabs (Likang Disinfectant H-Tech. Co., Shanghai, China). Eye lashes were covered with Steri-Strips (R1457; 3M Company, Pasadena, CA USA), the face draped (D1022; Cardinal Health, Los Angeles, CA USA), and a sterile wired lid speculum placed. Investigators themselves were sterile masked, capped, and gloved. All instruments were both disposable and suitable for human surgery or were autoclaved and cooled prior to usage. Throughout the procedure, the veterinary technician or head veterinarian at Beijing Institute of Xieerxin Biology Resource monitored the NHP in the room. Prior to regaining consciousness or at any sign of discomfort, NHPs were dosed with additional topical anesthetic and/or given additional intramuscular Zoletil 50 (1/3-1/2 of the initial dose). After imaging, the anterior chambers were flushed with Ringer's solution (RS), wounds hydrated, a 10-0 nylon suture placed to secure the wound, and topical 0.3% tobramycin/0.1% dexamethasone ointment (TobraDex; Alcon, Ft. Worth, TX, USA) applied. All NHP were monitored post-operatively daily and treated appropriately with no complications noted.

Aqueous Angiography

Aqueous angiography imaging was performed similar to as previously described^{18–21} but modified for intact eyes of living subjects. The NHP palpebral fissure precluded an inferior

approach and covered much of the ocular surface posterior to the limbus. Therefore, the first step was to place superior and inferior peripheral mid-depth corneal 8-0 prolene traction sutures (Ethicon, Somerville, NJ, USA) that were used to rotate the eye. This also meant that unlike prior publications^{18–20} with post-mortem eyes, simultaneous 360-degree appreciation of aqueous angiographic patterns around the limbus was not possible. Since the primary purpose of this study was to demonstrate aqueous angiography in intact eyes of living NHPs and to document potential segmental outflow patterns, this suture was necessary to move the eye for imaging different locations. Then, a Lewicky AC maintainer (BVI Visitec, Alcester, UK) was inserted through a 1 mm sideport (Alcon) into the anterior chamber from a temporal approach. All eyes studied were right eyes given orientation of the room and ethical guidelines to leave one non-manipulated eye in each NHP. Pharmaceutical grade RS (CR Double-Crane, Beijing, China), identical to what is used for human surgery, was introduced into the anterior chamber from a reservoir height set at ~10 inches above the eye to provide a gravity-delivered constant pressure of ~18.7 mm Hg.

Given the use of live animals, supine imaging was necessary. Heidelberg Engineering provided a prototype surgical FLEX module (mobile stand equipped with an arm) that allowed the standard clinical table-mounted Spectralis HRA+OCT (Heidelberg Engineering GmbH, Heidelberg, Germany) camera head to be suspended for supine imaging (Fig 1). The FLEX module allowed for stable three dimensional manipulations and positioning of the camera head relative to the eye utilizing multiple pivot joints. Alignment of the OCT/angiographic images along the z-axis were controlled by an integrated micro-manipulator.

From this position, the angiographer was placed in front of the eye, and confocal scanning laser ophthalmoscopic (cSLO) infrared images were taken to center the eye using a 55-degree lens and a 25 diopter focus. Fluorescent images were taken on **fluorescein capture mode** (excitation wavelength = 486 nm and transmission filter set at > 500 nm) or **ICG capture mode** (excitation wavelength = 786 nm and transmission filter set at > 800 nm) to establish the pre-injection background which appeared black. Alternatively, videos were taken. Pharmaceutical-grade 10% fluorescein (Fluorescite; Alcon) was diluted at room temperature in RS to 2.5%. Pharmaceutical grade ICG (Liaoning Tianyi Biopharmaceutical Company, Shenyang, Liaoning, China) was dissolved with solvent into a 2% stock solution and subsequently diluted in RS to 0.4%. These concentrations were chosen based on prior experience in enucleated pig and human eyes^{18–21} and because they have been described for clinical use at these concentrations in live humans as intraocular capsular stains for cataract surgery.²³

In cases of sequential delivery, ICG was first introduced for aqueous angiography at 18.7 mm Hg after gentle removal of aqueous humor without damage to intraocular tissues using a 1 ml syringe. This was then followed by fluorescein aqueous angiography in the same eye.

Anterior Segment Optical Coherence Tomography (OCT)

Anterior segment OCT^{18–20} (anterior segment module [Heidelberg Engineering, Germany] on Scleral mode) was concurrently conducted in two eyes with ICG aqueous angiography alone to determine if angiographically positive regions showed vessel anatomy compatible for AHO. Single line scans with a 15-degree scan angle (3.9 micron axial and 11 micron

lateral resolution; ~ 4.5 mm) were taken with oversampling (automated real-time = 20) in angiographically positive/negative regions.

Results

Aqueous Angiography in Living NHPs Likely Represents Aqueous Humor Outflow

Aqueous angiography in living and intact NHP eyes demonstrated branching patterns similar to previously published results in post-mortem eyes^{18–21}. Overlay of the fluorescein aqueous angiography signal on top of an infrared image clearly showed overlap of the fluorescent signal to the surface episcleral vein (Fig 2; NHP-A). In NHP-B, the superior portion of the eye posterior to the limbus (Fig. 3 A–C) showed a downward pointing fork-like structure with 4 arms. The superior-nasal portion of a separate NHP eye (NHP-C) showed more linear outflow patterns (Fig. 3 D/E). Anterior segment OCT in angiographically positive regions demonstrated strikingly more and larger intrascleral lumens (Fig. 3F/H/J, yellow and green arrowheads) compatible with AHO compared to angiographically negative regions. This was particularly obvious in the horizontal scan pattern, where the scan was taken across all four arms of the downward pointing fork (Fig. 3C) demonstrating 4 lumens on the OCT (Fig. 3H; green arrowheads). Note that small lumens were still seen in angiographically negative regions (Fig. 3 G/I; blue arrowheads) and may have represented other luminal structures in the sclera such as arteries.

Aqueous Angiography Demonstrated Segmental Patterns

Similar to post-mortem eyes^{18–21}, segmental angiographic patterns were seen in intact living NHP eyes. Regions of peri-limbal angiographic positivity (Figs 4 and 5; arrowheads) drained to distal areas (Figs 4 and 5; asterisks) and were intermixed with regions lacking an angiographic signal (Figs 4 and 5; arrows). Sequential aqueous angiography with ICG first followed by fluorescein (NHP-C) demonstrated similar but not identical patterns of regions with and without angiographic signal (Fig. 6; red arrows).

Aqueous Angiography Sometimes Demonstrated a Pulsatile Nature

Within a single and stable outflow structure, pulsatile flow sometimes was observed with ICG (Clip 1) or fluorescein (Clip 2) despite tracer delivery via a constant-pressure system. Heart rate was not synchronously monitored in relation to aqueous angiography, but rates of pulsations were counted in short video segments where pulsations were seen (9 video segments of 3–9 seconds in length including 4 distinct episcleral veins) demonstrating rates of 57–185 pulses per minute (average = 120 +/- 52 pulses per minute; mean +/- SD).

Aqueous Angiography Patterns Could Be Both Stable and Dynamically Change

Previously, segmental aqueous angiography patterns in post-mortem eyes always became more homogeneous over time because episcleral veins were disrupted by the enucleation process, and tracers delivered into the eye ultimately accumulated on the ocular surface^{18–21}. Tested in intact and living eyes, segmental patterns stayed more stable over time (Fig 7; NHP-C and NHP-F). However, at random intervals aqueous angiographic patterns also had the potential to become dynamic and actively change. For example, in NHP-B over 10 seconds of approximately evenly spaced single image acquisitions, an initially superior ICG

angiographic signal shifted nasally (Fig 8 A–J). Not only could regions without angiographic signal develop new signal (Fig. 8 [NHP-B] and Clip 3 [NHP-C using fluorescein]), but regions with angiographic signal could also diminish (Clip 4; NHP-B using ICG). Overall, during approximately 500 seconds of video imaging, a total of only 16 dynamic events were observed in any position of the eye. Dynamic change differed from pulsations in that the actual angiographic patterns physically shifted as opposed to pulsations where alterations in signal intensity were seen within a stable lumen. Defined as such, even during episodes of dynamic change, simultaneous pulsations could be seen as well (Clip 4; arrow).

Discussion

Real-time aqueous angiography of fluorescent tracer movement in intact eyes of live NHPs demonstrated segmental patterns that were pulsatile and dynamic. The potential for segmental AHO has been described in multiple systems. Outflow studies using microbeads or spheres have demonstrated segmental AHO in enucleated mammalian and live rodent eyes^{24–34}. Most of these observations have focused on the TM, and some have allowed for fine dissection of regions of higher or lower flow for careful biochemical and structural analyses^{31–34}. Aqueous angiography supported these past observations but was initially tested and developed in an enucleated system creating confounders related to using post-mortem eyes^{18–20}. Therefore, testing in intact eyes of living subjects was necessary to better understand clinically relevant AHO. In the current study, live aqueous angiography in a small number of NHPs replicated segmental patterns seen in enucleated eyes further supporting previous studies.

The use of different tracers for evaluating segmental AHO must be emphasized. Any tracer study is only as good as the tracer being employed. In other words, different patterns could emerge from different tracers based on their varying molecular characteristics of each tracer (molecular weight, charge, protein binding, etc.). For AHO, tracers that have been used include Q-dots or microspheres of different sizes (0.01 to 20 microns) which may have best modeled cellular or larger particulate movement^{25–34}. ICG has a molecular weight of ~775 g/mol; and, given its propensity for protein binding, may better model protein movement in the eye. Fluorescein^{18, 35} is a smaller molecule and has a molecular weight of ~332g/mol. Therefore, it more closely models the water movement component of aqueous humor. Because aqueous humor is complex and comprises many constituents (eg. cells, macromolecules, micromolecules, ions, water etc.), the aggregate similar observations of segmental AHO by different laboratories using different tracers with various molecular properties provide increased support for the concept of segmental AHO. Regarding, fluorescein and ICG, using enucleated human and cow eyes, similarities were established¹⁹ such that interventions could be placed between angiographies of the two dyes and assessed as a differential change²⁰. In the future, more quantitative methods will need to be developed to both quantify more or less segmentalization as well as to provide local flow descriptors such as volume, delay, or rate.

Pulsatile flow is an AHO characteristic that is traditionally observed via clear fluid and blood movement and exchange at the aqueous and episcleral vein junction^{36, 37}. Pulsatile

aqueous flow has been shown to be responsive to transient ocular changes including eye movement, IOP, or blinking^{17, 38}. Changes to pulsatile patterns have been linked to glaucoma with a greater number of classic Asher glass rod negative veins seen in disease^{36, 37}. Proposed mechanisms involve a cardiac basis such as systemic vasculature induced cyclical choroidal expansion acting like an intraocular piston¹⁷. Set-points have been proposed where pulsations appear only after intraocular pressure reach above a certain threshold¹⁷. More recently, phase-contrast OCT (PhS-OCT) has recorded optical phase information embedded in the OCT signal that allowed for greater sensitivity (as small as 0.26 nm) in sensing tissue movement¹⁵. This was in contrast to conventional OCT methods that utilized signal amplitude and structural border segmentation with motion tracking to follow movement. PhS-OCT has documented pulsatile AHO pathway structural movement in *ex vivo* model eyes^{14, 16} and live human subjects³⁹. Temporal analyses of live image acquisition found a synchronous relationship with a fixed time delay (~0.5 seconds) to heart rate as measured by a digital pulse³⁹.

With aqueous angiography results in living NHPs, pulsatile flow also was sometimes seen with a constant-pressure tracer non-pulsatile delivery system. While heart rate was not monitored in synchrony with aqueous angiography, pulsations rates (57–185 pulses per minute) did approximate normal heart rates of Rhesus macaques (resting: 70–180; exercise: 150–270 bpm)^{40, 41} suggesting a potential relationship. However, pulsations were not always observed. Since evaluating pulsations was not the initial purpose of this study, the device settings were established to maximize viewing of outflow vessels, and signal intensity saturation diminishing the dynamic range of aqueous angiography signal intensity may have limited the ability to discern pulsations. The presence of pulsations only during signal decrease of a dynamic change in clip 4 supported this. Additionally, while all efforts were made to hold the eye steady, transient investigator movements during imaging could have been a confounder or added noise to pulsatile flow. The presence of pulsations may also have been masked by individual cardiovascular or ocular set-point¹⁷ (see above) differences between individual subjects. Nevertheless, the presence of pulsatile flow is supported by the literature, deserves more dedicated angiographic study, and through methods such as aqueous angiography, investigators may be able to evaluate pulsatile features such as the set-point pressure in the future.

The real-time nature of aqueous angiography in the current study also enabled the observation of dynamic AHO patterns, a novel finding. Dynamic changes to the angiographic AHO patterns appeared to occur randomly such that it was not possible to consistently capture these moments since they were unpredictable and data acquisition in each session was limited by the software buffer. Nevertheless, the capability of regions without signal to develop AHO and for regions with angiographic signal to lose it makes intuitive sense as most organs are living, dynamic, and changing systems. The biology of what controlled this dynamism though is unclear. Regulation could be at the level of TM with changes to capacitance. Alternatively, vessel tone in the distal pathway (venous plexus, aqueous vein, or episcleral vein) could also modulate AHO patterns. The configuration of the distal outflow structure may also be important. The dynamic nature of AHO will be a future direction of investigation hopefully comparing normal to glaucoma eyes.

Several limitations in this study must be mentioned. First, NHP corneas were large and palpebral fissures small. A lid speculum was used and while necessary, could either introduce surface pressure to the eye or relieve it by supporting the lids. Also, even with a lid speculum, the only way to see posterior to the limbus was to place corneal traction sutures for eye rotation as described in the Methods. While routinely used in clinical ophthalmology surgery, traction sutures may have created unnatural force vectors during eye rotation. Normally, extraocular muscles insert greater than 5 mm posterior to the limbus⁴². While normal eye motion by extraocular muscle contraction is known to influence IOP^{17, 38}, the force vectors in this study were likely different from the usual configuration and a potential source of non-physiologic bias. Also, the traction suture was necessary because a major purpose of this study was to look for segmental AHO patterns (as in post-mortem eye results) in intact eyes of living NHPs. Therefore, the majority of imaging was done moving the eye with a traction suture to appreciate all regions close in time. While persistent imaging in one particular location would have been better for studying dynamic or pulsatile flow, imaging only in one spot would preclude knowing what was happening on the other side of the eye. During live human imaging in the future, a traction suture may not be needed, particularly if a patient can move their eye to command under topical anesthesia.

Additionally, introduction of tracers for aqueous angiography was routinely delivered into the anterior chamber. Aqueous humor normally arises from the sulcus space. Introduction of fluid into the anterior chamber is known to possibly and artifacticiously deepen the anterior chamber^{26, 43}. However, accessing and delivering any agent into the sulcus of an intact, living, and phakic eye is dangerous. There are risks for lens capsule perforation resulting in a lens particle glaucoma, sterile endophthalmitis (phacoanaphylaxis), or possible sulcus bleeds creating hyphemas or vitreous hemorrhages. Each of these are potentially visually devastating. Ethics board approval for such a maneuver was not granted in this study. Additionally, for patient care, most surgeons would be hesitant to adopt a technique that could lead to vision threatening complications for their patients. Therefore, since one of the goals of aqueous angiography was for translation to a patient-care environment (initially developed as a *bedside* to *bench* approach starting with adapting clinically available and FDA-approved devices/instruments for the lab), modeling fluid flow after introduction into the anterior chamber as opposed to the sulcus was and will be important.

In conclusion, aqueous angiography in a living NHP demonstrated segmental, pulsatile, and dynamic AHO. To the best of our knowledge this is the first demonstration of dynamic AHO pattern changes in intact eyes of living subjects. This new imaging technology opens new avenues of research for better understanding AHO. Clinically, it will be interesting to see how glaucoma affects the segmental, pulsatile, and dynamic characteristics seen here. Current pharmacological and surgical therapies in glaucoma could already be affecting these parameters. Future approaches may be devised to take advantage of these AHO characteristics as well.

Supplementary Material

Refer to Web version on PubMed Central for supplementary material.

Acknowledgments

Grant Support:

Funding for this work came from National Institutes of Health, Bethesda, MD (Grant Numbers K08EY024674 [ASH]; American Glaucoma Society (AGS) Mentoring for Physician Scientists Award 2014 [ASH]; AGS Young Clinician Scientist Award 2015 [ASH]; Research to Prevent Blindness Career Development Award 2016 [ASH]; an unrestricted grant from Research to Prevent Blindness (New York, NY); National Natural Science Foundation of China (NW; 81271005 and 81300767), Beijing Municipal Administration of Hospitals Clinical Medicine Development of Special Funding Support (NW; ZYLX201501); Beijing Scholars Program (NW); and China Health and Medical Development Foundation (NW). The funders had no role in study design, data collection and analysis, decision to publish, or preparation of the manuscript.

References

1. GRANT WM. Experimental aqueous perfusion in enucleated human eyes. *Arch Ophthalmol.* 1963; 69:783–801. [PubMed: 13949877]
2. Johnson M. What controls aqueous humour outflow resistance? *Exp Eye Res.* 2006; 82(4):545–57. [PubMed: 16386733]
3. Swaminathan SS, Oh DJ, Kang MH, Rhee DJ. Aqueous outflow: segmental and distal flow. *J Cataract Refract Surg.* 2014; 40(8):1263–72. [PubMed: 25088623]
4. Van Buskirk EM. Trabeculotomy in the immature, enucleated human eye. *Invest Ophthalmol Vis Sci.* 1977; 16(1):63–6. [PubMed: 832967]
5. Minckler D, Mosaed S, Dustin L, Ms BF. Trabectome (trabeculectomy-internal approach): additional experience and extended follow-up. *Trans Am Ophthalmol Soc.* 2008; 106:149–59. discussion 59–60. [PubMed: 19277230]
6. Ahuja Y, Ma Khin Pyi S, Malihi M, et al. Clinical results of ab interno trabeculotomy using the trabectome for open-angle glaucoma: the Mayo Clinic series in Rochester, Minnesota. *Am J Ophthalmol.* 2013; 156(5):927–35. e2. [PubMed: 23954209]
7. Craven ER, Katz LJ, Wells JM, Giamporcaro JE. Cataract surgery with trabecular micro-bypass stent implantation in patients with mild-to-moderate open-angle glaucoma and cataract: two-year follow-up. *J Cataract Refract Surg.* 2012; 38(8):1339–45. [PubMed: 22814041]
8. Samuelson TW, Katz LJ, Wells JM, et al. Randomized evaluation of the trabecular micro-bypass stent with phacoemulsification in patients with glaucoma and cataract. *Ophthalmology.* 2011; 118(3):459–67. [PubMed: 20828829]
9. Kagemann L, Wollstein G, Ishikawa H, et al. Identification and assessment of Schlemm's canal by spectral-domain optical coherence tomography. *Invest Ophthalmol Vis Sci.* 2010; 51(8):4054–9. [PubMed: 20237244]
10. Kagemann L, Wollstein G, Ishikawa H, et al. Visualization of the conventional outflow pathway in the living human eye. *Ophthalmology.* 2012; 119(8):1563–8. [PubMed: 22683063]
11. Li G, Farsiu S, Chiu SJ, et al. Pilocarpine-induced dilation of Schlemm's canal and prevention of lumen collapse at elevated intraocular pressures in living mice visualized by OCT. *Invest Ophthalmol Vis Sci.* 2014; 55(6):3737–46. [PubMed: 24595384]
12. Hann CR, Bentley MD, Vercnocke A, et al. Imaging the aqueous humor outflow pathway in human eyes by three-dimensional micro-computed tomography (3D micro-CT). *Exp Eye Res.* 2011; 92(2):104–11. [PubMed: 21187085]
13. Li P, Johnstone M, Wang RK. Full anterior segment biometry with extended imaging range spectral domain optical coherence tomography at 1340 nm. *J Biomed Opt.* 2014; 19(4):046013. [PubMed: 24752381]
14. Li P, Reif R, Zhi Z, et al. Phase-sensitive optical coherence tomography characterization of pulse-induced trabecular meshwork displacement in ex vivo nonhuman primate eyes. *J Biomed Opt.* 2012; 17(7):076026. [PubMed: 22894509]
15. Hariri S, Johnstone M, Jiang Y, et al. Platform to investigate aqueous outflow system structure and pressure-dependent motion using high-resolution spectral domain optical coherence tomography. *J Biomed Opt.* 2014; 19(10):106013. [PubMed: 25349094]

16. Sun YC, Li P, Johnstone M, et al. Pulsatile motion of trabecular meshwork in a patient with iris cyst by phase-sensitive optical coherence tomography: a case report. *Quant Imaging Med Surg.* 2015; 5(1):171–3. [PubMed: 25694967]
17. Johnstone M, Martin E, Jamil A. Pulsatile flow into the aqueous veins: manifestations in normal and glaucomatous eyes. *Exp Eye Res.* 2011; 92(5):318–27. [PubMed: 21440541]
18. Saraswathy S, Tan JC, Yu F, et al. Aqueous Angiography: Real-Time and Physiologic Aqueous Humor Outflow Imaging. *PLoS One.* 2016; 11(1):e0147176. [PubMed: 26807586]
19. Huang AS, Saraswathy S, Dastiridou A, et al. Aqueous Angiography with Fluorescein and Indocyanine Green in Bovine Eyes. *Transl Vis Sci Technol.* 2016; 5(6):5.
20. Huang AS, Saraswathy S, Dastiridou A, et al. Aqueous Angiography-Mediated Guidance of Trabecular Bypass Improves Angiographic Outflow in Human Enucleated Eyes. *Invest Ophthalmol Vis Sci.* 2016; 57(11):4558–65. [PubMed: 27588614]
21. Huang AS, Mohindroo C, Weinreb RN. Aqueous Humor Outflow Structure and Function Imaging At the Bench and Bedside: A Review. *J Clin Exp Ophthalmol.* 2016; 7(4)
22. Unwin, S. *The Laboratory Primate.* Wolfe-Coote, S., editor. San Diego, CA: Elsevier Science; 2005. v. Handbook on Experimental Animals
23. Jacobs DS, Cox TA, Wagoner MD, et al. Capsule staining as an adjunct to cataract surgery: a report from the American Academy of Ophthalmology. *Ophthalmology.* 2006; 113(4):707–13. [PubMed: 16581432]
24. Sabanay I, Gabelt BT, Tian B, et al. H-7 effects on the structure and fluid conductance of monkey trabecular meshwork. *Arch Ophthalmol.* 2000; 118(7):955–62. [PubMed: 10900110]
25. Chang JY, Folz SJ, Laryea SN, Overby DR. Multi-scale analysis of segmental outflow patterns in human trabecular meshwork with changing intraocular pressure. *J Ocul Pharmacol Ther.* 2014; 30(2–3):213–23. [PubMed: 24456518]
26. Battista SA, Lu Z, Hofmann S, et al. Reduction of the available area for aqueous humor outflow and increase in meshwork herniations into collector channels following acute IOP elevation in bovine eyes. *Invest Ophthalmol Vis Sci.* 2008; 49(12):5346–52. [PubMed: 18515571]
27. Lu Z, Overby DR, Scott PA, et al. The mechanism of increasing outflow facility by rho-kinase inhibition with Y-27632 in bovine eyes. *Exp Eye Res.* 2008; 86(2):271–81. [PubMed: 18155193]
28. Braakman ST, Read AT, Chan DW, et al. Colocalization of outflow segmentation and pores along the inner wall of Schlemm’s canal. *Exp Eye Res.* 2015; 130:87–96. [PubMed: 25450060]
29. Zhu JY, Ye W, Wang T, Gong HY. Reversible changes in aqueous outflow facility, hydrodynamics, and morphology following acute intraocular pressure variation in bovine eyes. *Chin Med J (Engl).* 2013; 126(8):1451–7. [PubMed: 23595376]
30. Zhu JY, Ye W, Gong HY. Development of a novel two color tracer perfusion technique for the hydrodynamic study of aqueous outflow in bovine eyes. *Chin Med J (Engl).* 2010; 123(5):599–605. [PubMed: 20367989]
31. Vranka JA, Bradley JM, Yang YF, et al. Mapping molecular differences and extracellular matrix gene expression in segmental outflow pathways of the human ocular trabecular meshwork. *PLoS One.* 2015; 10(3):e0122483. [PubMed: 25826404]
32. Keller KE, Bradley JM, Vranka JA, Acott TS. Segmental versican expression in the trabecular meshwork and involvement in outflow facility. *Invest Ophthalmol Vis Sci.* 2011; 52(8):5049–57. [PubMed: 21596823]
33. Cha ED, Xu J, Gong L, Gong H. Variations in active outflow along the trabecular outflow pathway. *Exp Eye Res.* 2016
34. Yang CY, Liu Y, Lu Z, et al. Effects of Y27632 on aqueous humor outflow facility with changes in hydrodynamic pattern and morphology in human eyes. *Invest Ophthalmol Vis Sci.* 2013; 54(8):5859–70. [PubMed: 23920374]
35. Loewen RT, Brown EN, Roy P, et al. Regionally Discrete Aqueous Humor Outflow Quantification Using Fluorescein Canalograms. *PLoS One.* 2016; 11(3):e0151754. [PubMed: 26998833]
36. Ascher, KW. *The Aqueous Veins.* In: Ritch, R., Caronia, RM., editors. *Classic Papers in Glaucoma.* Netherlands: Kugler Publications; 2000.
37. Thomassen TL, Perkins ES, Dobree JH. Aqueous veins in glaucomatous eyes. *Br J Ophthalmol.* 1950; 34(4):221–7. [PubMed: 15411485]

38. Coleman DJ, Trokel S. Direct-recorded intraocular pressure variations in a human subject. *Arch Ophthalmol*. 1969; 82(5):637–40. [PubMed: 5357713]
39. Li P, Shen TT, Johnstone M, Wang RK. Pulsatile motion of the trabecular meshwork in healthy human subjects quantified by phase-sensitive optical coherence tomography. *Biomed Opt Express*. 2013; 4(10):2051–65. [PubMed: 24156063]
40. de Lorge, J., Thach, JS. NASA. Rhesus Monkey Heart Rate During Exercise. Pensacola, Florida: NASA; 1972.
41. Wolfensohn, S., Lloyd, M. Handbook of Laboratory Animal Management and Welfare. 4. Oxford, UK: Wiley-Blackwell; 2013. Primates.
42. Ahmad, BU., Shah, G., Engelbrecht, N., et al. Chapter 24: Retinal Detachment Repair. New Delhi: The Health Sciences Publisher; 2015.
43. Ellingsen BA, Grant WM. The relationship of pressure and aqueous outflow in enucleated human eyes. *Invest Ophthalmol*. 1971; 10(6):430–7. [PubMed: 5578207]

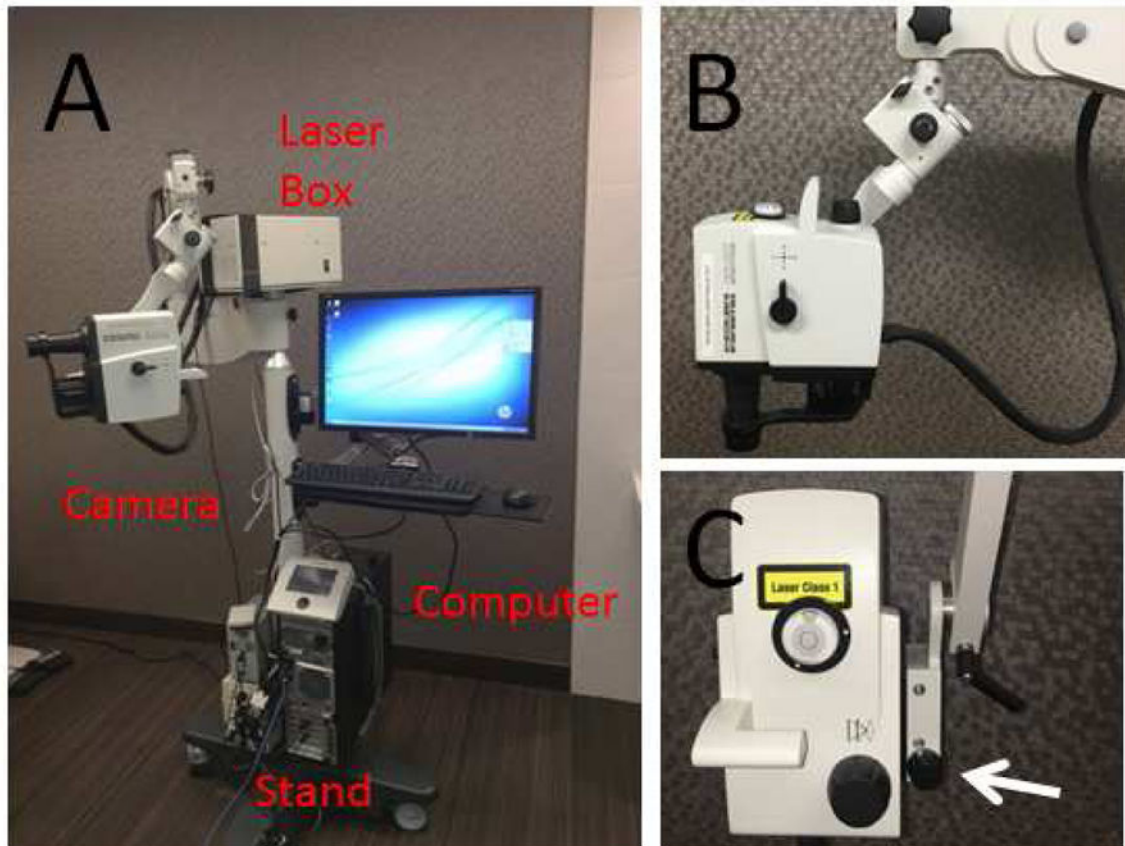


Figure 1. Heidelberg Engineering Flex Module

(A) The Flex Module suspended the camera head, disassembled from the standard table-top Spectralis, to allow for non-seated and non-upright image acquisition. (B) Seven pivot joints gave it maximum flexibility so that theoretically images could be taken sitting, supine, or prone with or without head down or up tilt. (C) A micro-manipulator allowed for precise z-axis movement (arrow). A 200-pound base in the stand provided stability and safety.

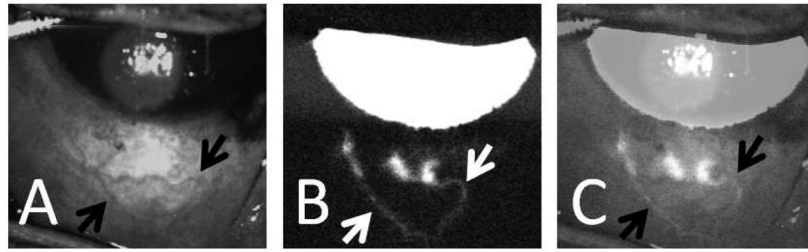


Figure 2. Aqueous Angiography in an Intact Living NHP Eye

(A) Infrared imaging of the inferior portion the NHP-A eye demonstrated surface episcleral veins (black arrows). (B) Aqueous angiography (fluorescein) in the same eye demonstrated three peri-limbal spots of angiographic signal that traced posterior (white arrows). (C) Overlay of images (A) and (B; 50% transparency setting using Photoshop CS5 v.12×32) showed good correspondence of angiographic signal to some of the episcleral vessels (black arrows).

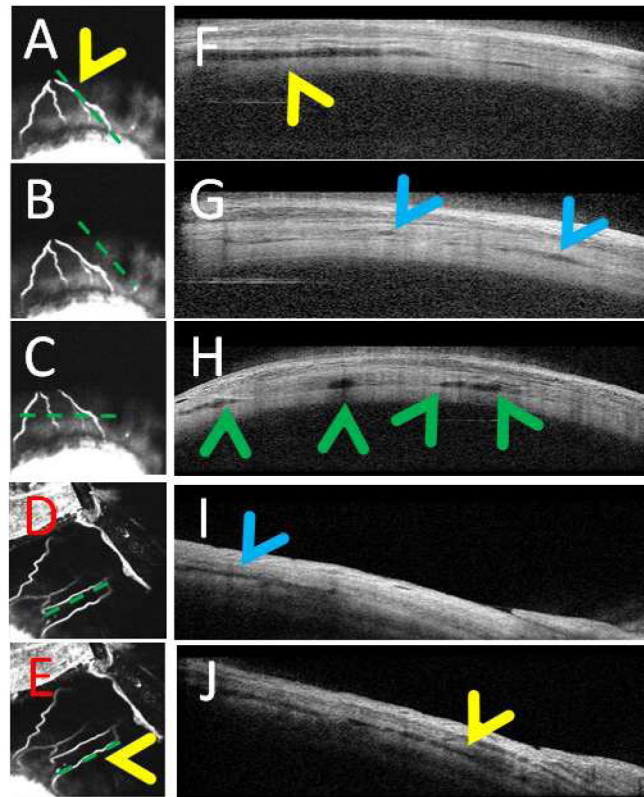


Figure 3. Aqueous Angiography and Anterior Segment Optical Coherence Tomography
 (A–C) Aqueous angiography (ICG) of the superior portion of the NHP-B eye showed an inferior pointing fork-like arrangement with 4 arms. (D/E) Aqueous angiography (ICG) of the superior-nasal portion of NHP-C eye showed a more linear arrangement. (F/H/J) Anterior segment OCT in angiographically positive areas (A/C/E) showed more intrascleral lumens (yellow and green arrowheads). (B/D) Angiographically negative regions showed (G/I; blue arrowheads) much less but still present lumens that many have corresponded to other intrascleral luminal structures such as arteries. Note that the horizontal anterior OCT scan pattern (C) cut across two angiographic arms on the left and near the root of another angiographic branch on the right corresponding to (H) four lumens on OCT (green arrowheads).

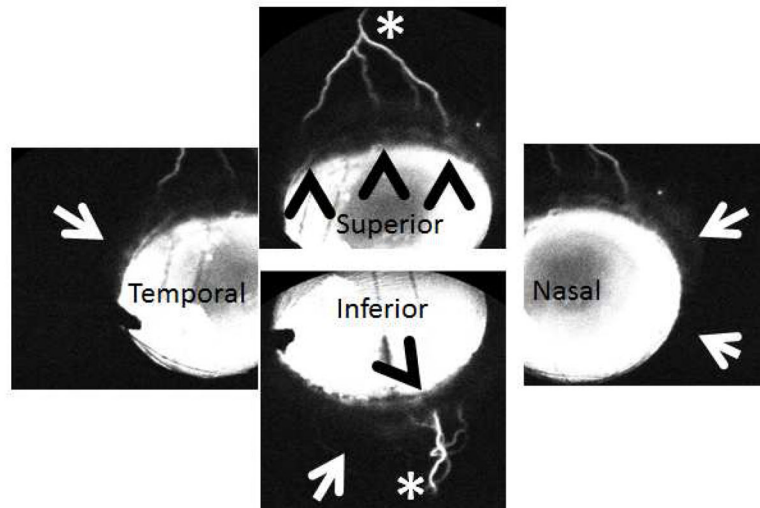


Figure 4. Aqueous Angiography Demonstrated Segmental Patterns (NHP-B)

Aqueous angiography looking at different quadrants of the eye demonstrated segmental patterns with some regions of peri-limbal angiographic signal (black arrowheads), intermixed with peri-limbal regions without signal (white arrows), leading to more distal angiographic signal (white asterisks).

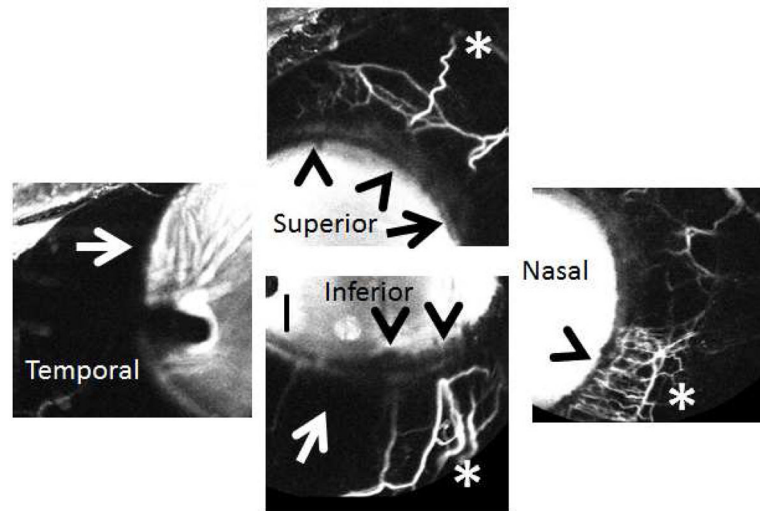


Figure 5. Aqueous Angiography Demonstrated Segmental Patterns (NHP-C)

Aqueous angiography looking at different quadrants of the eye demonstrated segmental patterns with some regions of peri-limbal angiographic signal (black arrowheads), intermixed with peri-limbal regions without signal (white and black arrows), leading to more distal angiographic signal (white asterisks).

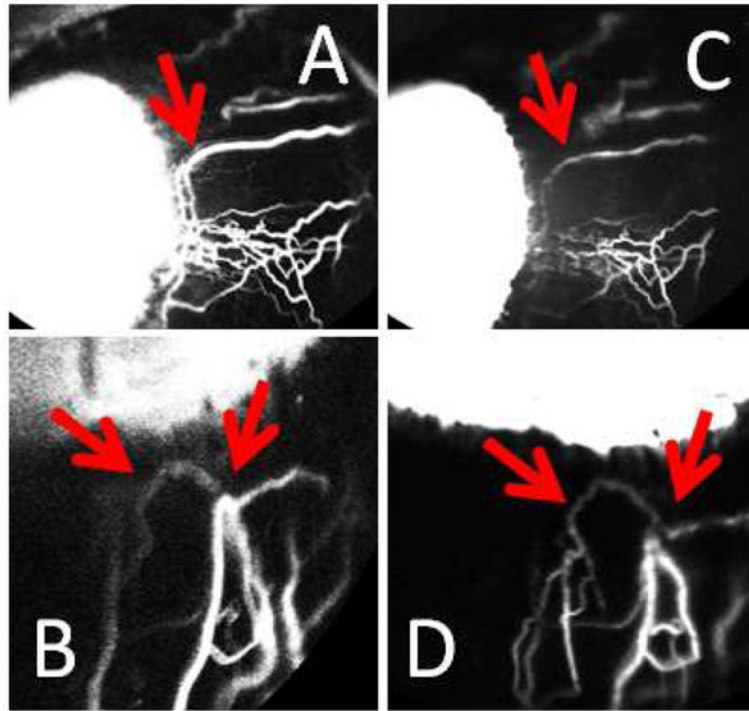


Figure 6. Sequential Aqueous Angiography with ICG and Fluorescein Demonstrated Similar Patterns

In one eye (NHP-C), sequential aqueous angiography was performed with ICG (A/B) followed by fluorescein (C/D). Like results in post-mortem human eyes, similar patterns were observed between the two dyes (red arrows).

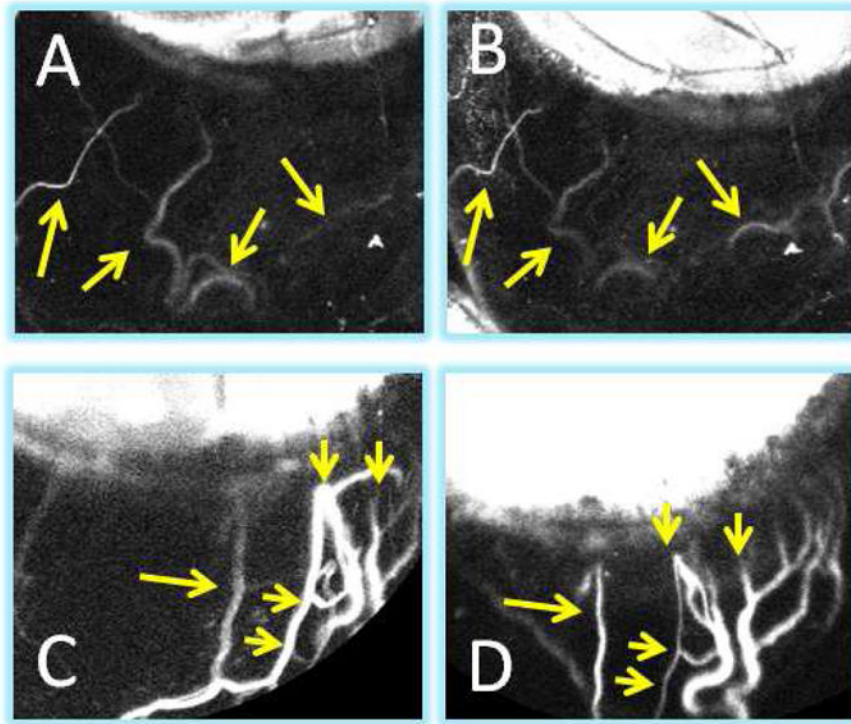


Figure 7. Aqueous Angiography Patterns in a Living Intact NHP Eye Demonstrated Stability Over Time

For the most part, unlike post-mortem eyes where the episcleral veins were severed open, in intact eyes, aqueous angiography patterns usually remained stable. ICG aqueous angiography in NHP-F at (A) 20 second was similar to that at (B) 2.5 minutes (yellow arrows). ICG aqueous angiography in NHP-C at (C) 2 minutes was similar to that at (D) 8 minutes (yellow arrows). (C/D) Note that these two images are slightly rotated when comparing.

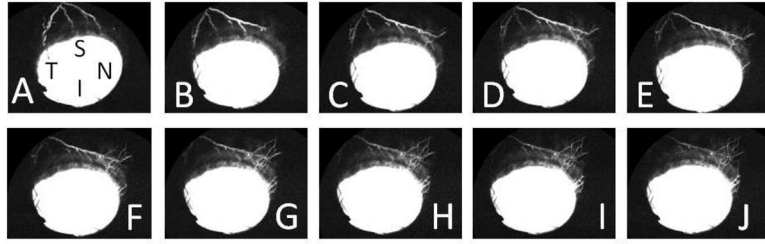


Figure 8. Aqueous Angiography Patterns in a Living Intact NHP Eye Were Sometimes Dynamic (A–J) While aqueous angiography patterns were mostly stable, sometimes, the patterns would dynamically change. In NHP-B, superior signal moved superior-nasal over approximately 10 seconds. S = superior, N = nasal, T= temporal, I = inferior.

Table 1

Details of NHP Subjects

Identification	Sex	Weight (kg)	Age (Years)
NHP-A	Male	12.3	15
NHP-B	Female	7.5	13
NHP-C	Male	10.5	25
NHP-D	Male	9	11
NHP-E	Male	8	10
NHP-F	Male	10.6	19

Author Manuscript

Author Manuscript

Author Manuscript

Author Manuscript